Chinese Chemical Letters 34 (2023) 107180

Contents lists available at ScienceDirect

Chinese Chemical Letters

journal homepage: www.elsevier.com/locate/cclet

Efficient removal of Cr(III)-carboxyl complex from neutral and high-salinity wastewater by nitrogen doped biomass-based composites

Li Song, Shichao Jing, Yixing Qiu, Fuqiang Liu*, Aimin Li

State Key Laboratory of Pollution Control and Resource Reuse, School of the Environment, Nanjing University, Nanjing 210023, China

ARTICLE INFO

Article history:
Received 17 November 2021
Revised 27 December 2021
Accepted 25 January 2022
Available online 1 February 2022

Keywords:
Biomass-based
Nitrogen doping
Adsorption
Complexed heavy metals
High-salinity wastewater

ABSTRACT

Heavy metals usually exist stably as the species of organic complexes in high-salinity wastewater. Therefore, their effective removal is challenging, especially when the initial pH is neutral. Herein, a novel nitrogen doped biomass-based composite (N-CMCS) was synthesized to remove the complexed heavy metal of Cr(III)-carboxyl. The maximum adsorption capacity of Cr(III)-Citrate (Cr-Cit) by N-CMCS under neutral pH (7.0) and high-salinity (200 mmol/L NaCl) condition was up to 2.50 mmol/g. And the removal performance remained stable after 6 times of regeneration. Combined with species and characterizations analysis, electrostatic attraction and hydrogen bonding were the main mechanisms for N-CMCS to remove Cr(III)-carboxyl complexes. Dynamic adsorption indicated N-CMCS column could treat about 1300 BV simulated wastewater and 350 BV actual wastewater with the concentration of effluent lower than 1.0 mg/L. Furthermore, N-CMCS could remove a variety of complexed heavy metal ions under neutral pH, indicating the great potential in practical application.

The leather industry occupies an important role in global economy, and its wastewater usually contains kinds of heavy metals, organics and compound pollutants, threatening the safety of ecosystem and public health [1–3]. Tannery wastewater contains not only chromium, which was mainly in the species of Cr(III), but also a variety of organic acid masking agents [4–6]. Although Cr(III) is generally considered to be less toxic than Cr(VI), inorganic Cr(III) and organic Cr(III) complexes can be oxidized to Cr(VI) not only by light induction in the natural environment, but also by chlorination in drinking water treatment [7,8]. In addition, the toxicity of Cr(III) to freshwater algae is higher than that of Cr(VI) under some specific conditions [9]. Meanwhile, the relevant wastewater pollutant discharge standards are becoming more and more stringent. Therefore, there is an urgent need for effective removal of Cr in tannery wastewater [10,11].

Among many methods, chemical precipitation is widely used due to the simplicity and economy [12–14]. However, there is still a large amount of Cr (10–20 mg/L) in the precipitated water, which is higher than China's maximum contaminant level (MCL) [15,16]. Since most of the free Cr(III) and weakly complexed Cr(III) are removed during precipitation process, the remaining Cr(III) complexed strongly with organic ligands usually exists as anionic or neutral molecules, which greatly increases the difficulty of removal due to the stability in a wide pH range [4,17].

The treatment methods for complexed heavy metals mainly include advanced oxidation processes (AOPs), metal ion replacement and adsorption. AOPs usually oxidize organic ligands by active oxygen species to release heavy metal ions for advanced treatment [18–20]. However, Cr(III) will be oxidized to Cr(VI) when oxidizing ligands of Cr(III)-carboxyl complex [7,21]. The metal ion replacement method replaces the target ion by using another ion with stronger complexing ability and Fe(III) is mostly used [5]. Unfortunately, due to the kinetic inertness of water exchange (such as $Cr(H_2O)_6^{3+}$, $t_{1/2} = 81.6$ h at 298.15 K), the complexation and decomposition rate of Cr(III) complexes is very slow, resulting in low efficiency of replacing Cr(III) with Fe(III) [22–24]. In comparison, the adsorption method is effective due to the simple operation, economics and no secondary pollution [25–27]. The adsorbents reported so far are mostly magnetic Fe_3O_4 nanomaterials modified with organic acids or biomass, which usually have a low point of zero charge (PZC), and the best applicable pH is acidic [10,28-30]. The mechanism for removing complexed Cr(III) mainly includes electrostatic attraction and surface complexation. However, the actual precipitated water has a neutral and alkaline pH, and Cr(III)-carboxyl complexes mainly exists as neutral molecules and negatively charged ions. Since neutral molecules are not charged, they are difficult to remove by electrostatic attraction [4]. Also, the reduction of zeta potential under alkaline conditions will inhibit the

* Corresponding author.
E-mail address: lfq@nju.edu.cn (F. Liu).

https://doi.org/10.1016/j.cclet.2022.01.073
1001-8417/

removal efficiency for negatively charged complexed ions. In addition, the coexistence of high concentration inorganic salt ions will adversely affect non-specific effects such as electrostatic interaction [26]. Therefore, it is urgent to develop new adsorbents with high adsorption capacity and anti-interference to remove Cr(III)-carboxyl complexes.

Sodium carboxymethyl cellulose (CMCS) is rich in hydroxyl and carboxylate, and has a wide range of sources and low price [31]. However, the negatively charged CMCS is not conducive to the electrostatic adsorption of complexed heavy metal anions. Considering that polyamines contain many amine groups and have high PZC, which can bind metal ions by coordination, electrostatic and hydrogen bond interactions [32]. As a result, it is expected that modified CMCS with polyamines can increase the positive charge density, promote the adsorption for complexed ions. Moreover, the double network structure constructed by two components can improve the mechanical stability. In this work, nitrogen-doped biomass-based composite (N-CMCS) was prepared, and the removal characteristics and mechanisms for Cr(III)-carboxyl complexes in high-salinity wastewater were investigated based on batch experiments and series of characterizations.

The preparation method of N-CMCS was the same as the method described in our previous work [33]. In short, CMCS and polyethyleneimine (PEI) were dissolved in water to form mixed solutions, then the crosslinking agent of epichlorohydrin (ECH) was added. After stirring evenly, it was heated at 60 °C for 4 h for reaction, and then washed several times with ethanol and ultrapure water to obtain N-CMCS.

$CrCl_3$ and trisodium citrate dihydrate (Cit) were mixed at a molar ratio of 1:1 to prepare Cr-Cit stock solution, and the pH was adjusted to 5 and maintained at 60 °C for 24 h. For batch experiments, 0.25 g of N-CMCS was placed in 30 mL of Cr-Cit solution with an initial pH of 7 and different coexisting NaCl concentrations (0, 50, 100, 200, 400 mmol/L) at 25 °C and 160 rpm for 24 h. Then inductively coupled plasma emission spectrometry (ICP-OES) (iCAP 8000) was used to determine the concentration of metal ions. To investigate the effect of pH, HCl and NaOH was used to adjust the pH of solution to 2–10. For adsorption isotherm experiments, N-CMCS was placed in solution with the initial concentration of 0.5–6.0 mmol/L for Cr-Cit and 200 mmol/L for coexisting NaCl. For the effect of other coexisting inorganic anions, NO_3^- and SO_4^{2-} were selected for test. Furthermore, the removal capacity for other complexed metal ions was also investigated, and the initial concentration was set to 1 mmol/L. For regeneration experiment, N-CMCS reached adsorption equilibrium was regenerated with 0.1 mol/L HCl and then proceeded to next cycle. For dynamic experiment, 5.25 g of N-CMCS was placed in the fixed column (100 mm in length and 10 mm in diameter). The water was pumped into the column with the rate of 2 BV/h. The basic component parameters of simulated and real wastewater were presented in Table S1 (Supporting information). According to China's emission standards (GB21900–2008) [34], the MCL value of Cr(III) in the effluent was set to 1.0 mg/L. The species analysis was carried out using Visual MINTEQ 3.1. Characterizations of N-CMCS were performed after freeze-drying. Thermo Scientific Nicolet iS5 (USA) spectrometer and Escalab 250 Xi (USA) were used for determination of ATR-FTIR and XPS analysis.

Firstly, with NaCl as a representative, the effect of solution salinity on adsorption of Cr-Cit by N-CMCS was investigated (Fig. 1a). Without the coexistence of NaCl, the adsorption capacity of Cr-Cit was the highest, as high as 2.02 mmol/g. But with the gradual increase of NaCl concentration, the removal ability for complexed Cr decreased, and the inhibition ratios were 14.52%, 22.87%, 41.12%, 51.22% and 61.01%, respectively. Although the electrostatic attraction between N-CMCS and Cr-Cit was almost completely shielded when the concentration of NaCl was as high as 400 mmol/L, the adsorption capacity was still maintained at 0.79 mmol/g. It indicated that there are other mechanisms besides electrostatic attraction, which will be discussed in detail later. Considering the salinity in actual wastewater, 200 mmol/L was selected for subsequent experiments.

The effect of pH was presented in Fig. 1b. Without the coexistence of NaCl, the adsorption capacity of Cr-Cit gradually increased and reached the maximum at pH of 5 in the pH range of 2–5. With the further increase of pH, the removal capacity decreased significantly, and the adsorption capacity at pH of 10 decreased by 54.90% compared with that at pH of 5. When 200 mmol/L NaCl coexisted, the adsorption behavior showed similar trend, but the dependence on pH was significantly reduced, and the adsorption capacity changed less in the pH range of 4–8. Even at pH of 8, the adsorption capacity only decreased by 9.74% compared with that of at pH of 5. Combined with zeta potential (Fig. S1 in Supporting information), N-CMCS had a PZC exceeded 9. When pH $<$ PZC, the positive charge on N-CMCS could remove complexed ions through electrostatic attraction. As the pH rose, the positive charge density on N-CMCS declined, and the electrostatic attraction was suppressed then. But even at pH of 10 ($>$ PZC), the adsorption capacity of Cr-Cit was still 0.57 mmol/g, indicating that there were other mechanisms besides the main electrostatic attraction. Considering that the pH of the actual precipitation water is neutral and alkaline, pH 7 was selected for subsequent experiments. Furthermore, the final pH was measured (Fig. S2 in Supporting information). When pH $<$ 7, the final pH after adsorption was slightly higher than the initial pH, while for pH $>$ 7, the change trend was totally opposite. It was mainly caused by the protonation and deprotonation of the carboxylate of citrate under different pH conditions. The reduced pH of solution was beneficial to removal for Cr-Cit, resulting in high removal capacity in a wide pH range.

The adsorption isotherm curves and related fitting parameters were presented in Fig. 1c. When the initial concentration increased from 0.5 mmol/L to 6.0 mmol/L, the adsorption capacity of Cr-Cit at 288, 298 and 318 K increased by 55.67%−213.64%, 53.49%−203.41%, 48.63%−189.02%, respectively. The adsorption isotherm data was fitted by Langmuir and Freundlich models (Table S2 in Supporting information). According to correlation coefficient R^2, the isothermal adsorption of Cr-Cit was more suitable for Freundlich model, indicating that Cr-Cit was covered on the heterogeneous surface of N-CMCS through multilayer adsorption. The calculated maximum adsorption capacity (Q_m) based on Langmuir model was 2.50 mmol/g at 298 K. As for adsorption kinetic behavior (Fig. S3 in Supporting information), the fitting models (Table S3 in Supporting information) exhibited a pseudo-second-order rate constant of 0.005 g $mmol^{-1}$ min^{-1}. The data of thermodynamic calculation showed that both ΔH^0 and ΔS^0 was greater than zero, indicating the remove of Cr-Cit by N-CMCS was a process of endothermic and entropy drive, and heating was conducive to adsorption. $\Delta G^0 < 0$ indicated that this process was spontaneous. Besides, ΔG^0 gradually decreased with increasing temperature, implying that heating could promote the adsorption of Cr-Cit (Table S4 in Supporting information).

The comparison of Q_m with reported works was displayed in Fig. 1d and Table S5 (Supporting information). The adsorbents reported were mostly Fe_3O_4 magnetic nanomaterials modified with organic acids or biomass [10,28-30,35-37]. However, the optimal pH was acidic, and Q_m of complexed Cr(III) needed to be improved. In comparison, Q_m of Cr-Cit by N-CMCS was up to 5.42 mmol/g at pH of 4 (Fig. S4 and Table S6 in Supporting information). Even at pH of 7, Q_m of Cr-Cit was still up to 2.50 mmol/g, which was much higher than that of the reported in salt-free system. It demonstrated that N-CMCS was an advantageous material for removing complexed Cr(III).

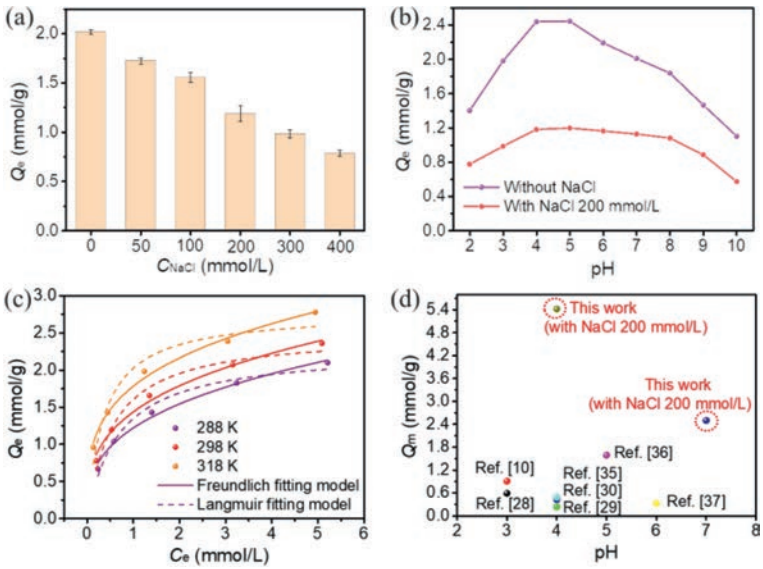

Fig. 1. The effect of (a) NaCl and (b) pH on removal for Cr-Cit, (c) the adsorption isotherms of Cr-Cit and (d) performance comparison with reported works on removal of complexed Cr(III).

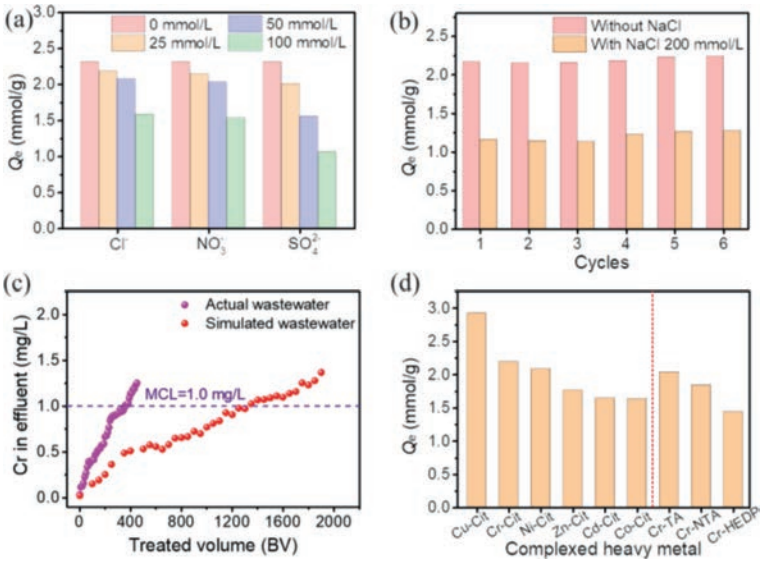

Fig. 2. (a) The effect of inorganic anions on Cr-Cit removal, (b) recycling performance of N-CMCS in different systems, (c) removal of simulated and actual wastewater with N-CMCS column and (d) the adsorption capacity of other heavy metal complexes.

The effect of coexisting inorganic ions was displayed in (Fig. 2a). The inhibitory followed the rule of SO_4^{2-} > NO_3^- > Cl^-, and the inhibition ratios were 13.14%–53.78%, 7.17%–33.50%, 5.40%–31.45%, respectively. The inhibitory effect of coexisting anions was mainly due to the competition with Cr-Cit anions, in which SO_4^{2-} had more negative charges and occupied more cation active sites on N-CMCS, thus, the strongest inhibitory effect was caused [38,39].

The N-CMCS after reaction was regenerated by HCl and subjected to next cycle (Fig. 2b). Regardless of the presence of NaCl, the adsorption capacity of Cr-Cit did not show any decreasing trend after 6 cycles, indicating it had good stability, which was conducive to practical application. Moreover, the applicability of N-CMCS to remove Cr(III) complex in simulated and actual high-salinity wastewater was investigated by dynamic adsorption experiment (Fig. 2c). N-CMCS could continuously produce about 1300 BV and 350 BV of water with the concentration of Cr lower than 1.0 mg/L for simulated and actual wastewater respectively, which implied the great potential in actual application.

The removal performance for other complexed heavy metals was investigated (Fig. 2d). Obviously, the adsorption capacity of Cu-Cit was the highest, which was up to 2.93 mmol/g. While it was the lowest for Co-Cit, but was still more than 1.60 mmol/g. This was mainly related to the species distribution (Figs. S5 and S6 in Supporting information) and chemical properties of N-CMCS. Specifically, N-CMCS contained many amine groups, and the formation of ternary complexes could also remove complexed Cu. Similarly, N-CMCS could also remove Cr(III) complexed with other organic acid ligands. Among them, the adsorption capacity of Cr-Cit was the largest, and for Cr-HEDP was the lowest, but it could also reach up to 1.45 mmol/g. In short, N-CMCS had good removal ability for various complexed metal ions.

In order to clarify the mechanism, the removal performance for Cr(III) and citrate in the non-complexed system was compared (Fig. 3a). The adsorption capacity of Cit by N-CMCS was only 0.47 mmol/g, which was due to the fact that Cit mainly existed as Cit^{3-} and $HCit^{2-}$ under neutral condition (Fig. S7 in Supporting in-

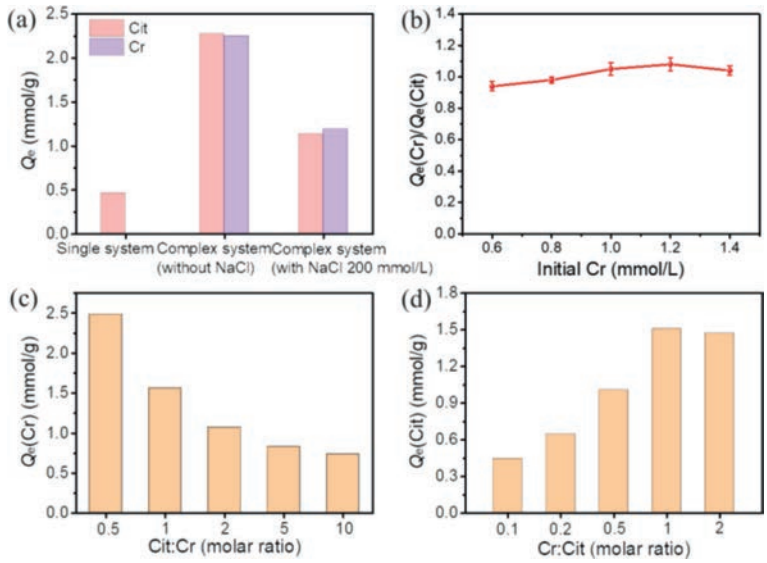

Fig. 3. (a) The adsorption capacity of Cr and Cit in different systems, (b) effect of initial concentration of Cr on molar ratio of residual Cr to Cit, effect of (c) Cit:Cr and (d) Cr:Cit on removal for Cr and Cit.

formation). When the total number of cation sites on N-CMCS was the same, the negative charge of ions was higher, and the more sites they occupied, resulting in lower adsorption capacity. After complexing with Cr(III), the main species of Cit were $CrH_{-1}Cit^{-}$ and CrCit. The reduction of negative charge saved the cationic active sites on N-CMCS, thereby increasing the adsorption capacity of Cit. Moreover, CrCit could also be adsorbed via hydrogen bonding between hydroxyl and amine groups since it was electrically neutral. For Cr(III), 78.51% was $Cr(OH)_3$ precipitation at pH of 7. Even at pH of 5, the adsorption capacity of Cr(III) by N-CMCS was only 0.09 mmol/g (Fig. S8 in Supporting information), which was mainly due to electrostatic repulsion between the positively charged N-CMCS surface and $CrOH^{2+}$. However, when Cr(III) was complexed with Cit, the adsorption capacity of complexed Cr was almost equivalent to that of Cit regardless of the presence or absence of NaCl. Also, the effect of different initial Cr concentration on the ratio of Q_{Cr} to Q_{Cit} was further investigated (Fig. 3b). When the concentration of Cr increased from 0.6 mmol/L to 1.4 mmol/L, Q_e(Cr)/Q_e(Cit) basically stabilized at 1, indicating that Cr and Cit were adsorbed on N-CMCS in an integral form.

For deep investigation, the effect of molar ratio on adsorption capacity was also tested (Figs. 3c and d). When the molar ratio of Cit:Cr grow from 1 to 10, the adsorption capacity of Cr declined significantly. It was mainly owing to the excess Cit existed as anions, which would compete with $CrH_{-1}Cit^{-}$, resulting in low utilization efficiency of active sites (Fig. S9 in Supporting information). When the molar ratio of Cit:Cr was 0.5, excess Cr(III) would generate precipitation (Fig. S10 in Supporting information), resulting in a higher apparent adsorption capacity than that of when Cit:Cr was 1. As the molar ratio of Cr:Cit rose from 0.1 to 1, the adsorption capacity of Cit also increased markedly, but remained basically unchanged when molar ratio exceeded 1. In summary, excessive Cit would compete with complexed Cr for active sites through electrostatic interaction, but excessive Cr had little effect on removal of Cit, so the adsorption of Cr-Cit by N-CMCS was mainly related to Cit.

The ATR-FTIR spectra of N-CMCS were exhibited in Fig. S11 (Supporting information). The peaks at 1586, 1374 and 1051 cm^{-1} corresponded to the peaks of COO^{-} asymmetric stretching vibration, COO^{-} symmetric stretching vibration and C=O stretching vibration, respectively. After adsorption of Cr-Cit, the peak corresponding to COO^{-} was significantly enhanced. In addition, the stretching vibration peak of O-H at 3284 cm^{-1} was also prominently enhanced, implying the formation of hydrogen bonds [40]. Combined with XPS spectra, the characteristic peak of Cr 2p appeared in the wide scan spectrum (Fig. 4a) after adsorption of Cr-Cit. In addition, the peaks at 585.6 and 576.1 eV in deconvolution spectra of Cr 2p (Fig. 4b) belong to Cr(III) [41], indicating that Cr-Cit was adsorbed on N-CMCS and had no redox effect with N-CMCS. In C 1s spectra (Fig. 4c), the peaks at 285.8, 284.7 and 283.3 eV corresponded to C−O, C−C and C−N, respectively [33]. After adsorption of Cr-Cit, a characteristic peak of C=O appeared at 288.1 eV with a molar ratio of 7.29%. Moreover, the molar ratio also ascended from 24.55% to 25.74% for C−O peak, but reduced from 23.58% to 13.30% for C−N peak. It was mainly due to the adsorption of citrate rich in hydroxyl and carboxylate, which caused an increase in the proportion of oxygen-containing chemical bonds. The three peaks in the N 1s spectra (Fig. 4d) are $-NH_2^{+}-/-NH_3^{+}$ at 401.4 eV, −NH−/$-NH_2$ at 399.0 eV, and N−C at 397.6 eV [42]. After adsorption, the molar ratio of $-NH_2^{+}-/-NH_3^{+}$ and −NH−/$-NH_2$ both rosed, from 19.93% to 29.75% and 46.76% to 53.24%, respectively, while decreasing from 33.31% to 17.01% for N−C. It implied the hydroxyl groups of citrate that were not involved in the coordination with Cr(III) formed hydrogen bonds with amine groups of N-CMCS.

To investigate the ratio of electrostatic attraction and hydrogen bonding, NaCl was selected as a representative for exploration the effect of ion strength on Cr-Cit removal (Fig. S12 in Supporting information). As the concentration of NaCl increased from 0 mmol/L to 800 mmol/L, the adsorption capacity of Cr-Cit decreased from 2.02 mmol/g to 0.27 mmol/g, and remained stable at 1000 mmol/L. When without NaCl, Cr-Cit was removed *via* electrostatic attraction and hydrogen bonding by N-CMCS. When NaCl coexisted, Cl^{-} could be adsorbed to cation sites on N-CMCS, thereby shielding the active sites of Cr-Cit and weakening the electrostatic attraction. When the concentration of NaCl was 1000 mmol/L, the electrostatic sites on N-CMCS were almost completely shielded, and Cr-Cit was mainly removed *via* hydrogen bonding. Based on the adsorption capacity of 0.27 mmol/g caused by hydrogen bonding, the adsorption capacity caused by electrostatic attraction was calculated as 1.75 mmol/g. Therefore, the ratio of electrostatic attraction and hydrogen bonding was 6.48.

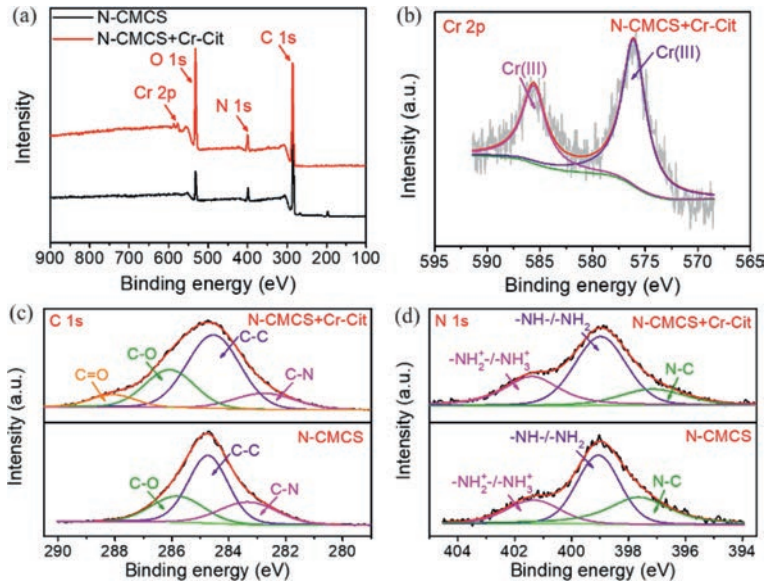

Fig. 4. XPS spectra of (a) wide scan, (b) Cr 2p, (c) C 1s and (d) N 1s before and after adsorption of Cr-Cit by N-CMCS.

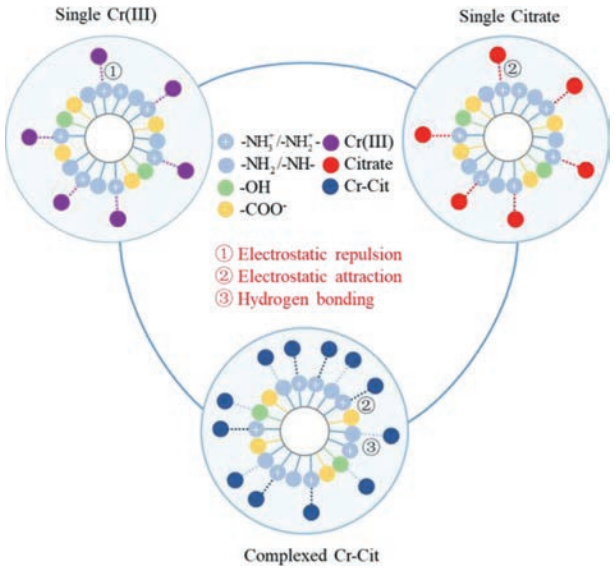

Fig. 5. The removal mechanism of Cr-Cit by N-CMCS.

In summary, N-CMCS could remove Cr-Cit efficiently, even under neutral and high-salinity conditions. The adsorption mechanism of Cr-Cit was mainly based on electrostatic attraction and hydrogen bonding (Fig. 5). Under neutral condition, the positively charged surface of N-CMCS could bind $CrH_{-1}Cit^{-}$ ions through electrostatic attraction. As the process progressed, the surface of N-CMCS appeared electrically neutral, and the neutral amine groups could further bind CrCit molecules through hydrogen bonding. Furthermore, N-CMCS exhibited good anti-interference and regeneration stability. Our research presented that N-CMCS had application potential for removal of complexed heavy metal ions.

Declaration of competing interest

The authors declare that they have no known competing financial interests or personal relationships that could have appeared to influence the work reported in this paper.

Acknowledgment

The authors gratefully acknowledge the support provided by the National Natural Science Foundation of China (No. 51522805).

Supplementary materials

Supplementary material associated with this article can be found, in the online version, at doi:10.1016/j.cclet.2022.01.073.

References

[1] F. Younas, N.K. Niazi, I. Bibi, et al., J. Hazard. Mater. 422 (2022) 126926.
[2] A.B. Mpofu, O.O. Oyekola, P.J. Welz, J. Clean Prod. 296 (2021) 126490.
[3] G.Y. Zheng, L.X. Zhou, S.M. Wang, Environ. Sci. Technol. 43 (2009) 4151–4156.
[4] Y.L. Tang, J.T. Zhao, J.F. Zhou, et al., Water Res. 178 (2020) 115807.
[5] M. Roverso, V. Di Marco, G. Favaro, et al., Chemosphere 264 (2021) 128487.
[6] B. Reyes-Romero, A.N. Gutierrez-Lopez, R. Hernandez-Altamirano, et al., J. Environ. Chem. Eng. 9 (2021) 104626.
[7] R.N. Dai, C.Y. Yu, J. Liu, et al., Environ. Sci. Technol. 44 (2010) 6959–6964.
[8] M. Chebeir, H.Z. Liu, Environ. Sci. Technol. 50 (2016) 701–710.
[9] D.A.L. Vignati, J. Dominik, M.L. Beye, et al., Ecotoxicol. Environ. Saf. 73 (2010) 743–749.
[10] J.H. Wang, Y. Chen, T.T. Sun, et al., Ecotoxicol. Environ. Saf. 209 (2021) 111858.
[11] D.D. Wang, Y.X. Ye, H. Liu, et al., Chemosphere 193 (2018) 42–49.
[12] S.J. Yu, H.W. Pang, S.Y. Huang, et al., Sci. Total Environ. 800 (2021) 149662.
[13] S. Zhang, J.Q. Wang, Y. Zhang, et al., Environ. Pollut. 291 (2021) 118076.
[14] L.P. Liang, F.F. Xi, W.S. Tan, et al., Biochar 3 (2021) 255–281.
[15] C.Q. Zhao, W.Y. Chen, Environ. Sci. Pollut. Res. 26 (2019) 26102–26111.
[16] Z. Song, C.J. Williams, R.G.J. Edyvean, Water Res. 34 (2000) 2171–2176.
[17] D.D. Wang, S.Y. He, C. Shan, et al., J. Hazard. Mater. 316 (2016) 169–177.
[18] B. Jiang, Q.H. Niu, C. Li, et al., Appl. Catal. B: Environ. 272 (2020) 119002.
[19] C.S. Shen, H. Li, Y.Z. Wen, et al., Chem. Eng. J. 383 (2020) 123105.
[20] H.R. Ma, Q. Wang, Y.Y. Hao, et al., Chemosphere 250 (2020) 126214.
[21] X.F. Huang, X.R. Wang, D.X. Guan, et al., Environ. Sci. Pollut. Res. 26 (2019) 8516–8524.
[22] Y.X. Ye, C. Shan, X.L. Zhang, et al., Environ. Sci. Technol. 52 (2018) 10657–10664.
[23] Y.X. Ye, Z. Jiang, Z. Xu, et al., Water Res. 126 (2017) 172–178.
[24] F.C. Xu, H.R. Krouse, T.W. Swaddle, Inorg. Chem. 24 (1985) 267–270.
[25] X.F. Lou, Y.N. Wu, D.M. Kabtamu, et al., J. Environ. Chem. Eng. 9 (2021) 104932.
[26] X.L. Zhang, P. Huang, S.Y. Zhu, et al., Environ. Sci. Technol. 53 (2019) 5319–5327.
[27] Y. Zhu, W.H. Fan, T.T. Zhou, et al., Sci. Total Environ. 678 (2019) 253–266.
[28] J.H. Wang, X.H. Tong, Y. Chen, et al., Microporous Mesoporous Mat. 303 (2020) 110262.
[29] J.H. Wang, Y. Chen, N. Liu, et al., Chin. J. Inorg. Chem. 36 (2020) 1249–1258.
[30] J.H. Wang, M. Mao, S. Atif, et al., React. Funct. Polym. 156 (2020) 104720.
[31] M. Sadeghi, Z. Moghimifar, H. Javadian, et al., J. Hazard. Mater. 417 (2021) 126038.
[32] C. Ling, X.Y. Li, Z.Y. Zhang, et al., Environ. Sci. Technol. 50 (2016) 10015–10023.
[33] L. Song, F.Q. Liu, C.Q. Zhu, et al., Chem. Eng. J. 369 (2019) 641–651.

[34] China EPA, Emission standard of pollutants for electroplating, 2008, GB21900-2008.
[35] J.H. Wang, S. Atif, D. Zhang, Environ. Technol. Innov. 20 (2020) 101088.
[36] R.Q. Ma, T. Wang, T.B. Huang, et al., J. Mol. Liq. 312 (2020) 113432.
[37] W. Zhang, X.Y. Ma, R. Li, et al., Colloid Surf. A-Physicochem. Eng. Asp. 625 (2021) 126819.
[38] F.L. Liu, S. Hua, C. Wang, et al., Chemosphere 279 (2021) 130539.
[39] F.L. Liu, S. Hua, C. Wang, et al., Chemosphere 287 (2022) 132199.
[40] C.H. Ji, D.W. Wu, J.H. Lu, et al., Water Res. 189 (2021) 116599.
[41] C.Q. Zhu, F.Q. Liu, Y.H. Zhang, et al., Chem. Eng. J. 306 (2016) 579–587.
[42] J.J. Wang, Z.K. Li, J. Hazard. Mater. 300 (2015) 18–28.